

# Coupled Nanomechanical Motions: Metal-Ion-Effected, pH-Modulated, Simultaneous Extension/Contraction Motions of Double-Domain Helical/Linear Molecular Strands

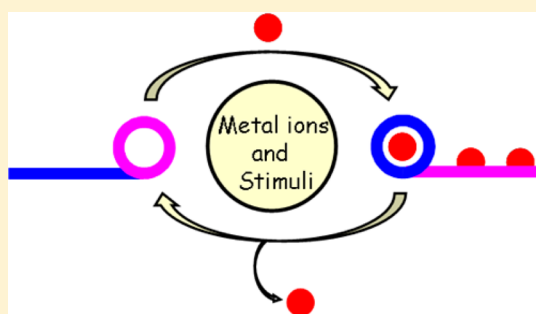
Adrian-Mihail Stadler<sup>\*,†,‡</sup> and Jean-Marie P. Lehn<sup>\*,†</sup>

<sup>†</sup>Laboratoire de Chimie Supramoléculaire, Institut de Science et d'Ingénierie Supramoléculaires, Université de Strasbourg, 8 Allée Gaspard Monge, Strasbourg, 67000, France

<sup>‡</sup>Institut für Nanotechnologie (INT), Karlsruhe Institut für Technologie (KIT), 76344 Eggenstein-Leopoldshafen, Germany

**S** Supporting Information

**ABSTRACT:** A new class of shape-enforced synthetic polyheterocyclic molecular strands, containing both a helical and a linear domain, has been designed and synthesized. On reaction with Pb(II), under the effect of cation binding to the coordination subunits, the helical section unfolds into a linear shape in the complex and the linear domain folds into a helical ligand wrapped around the bound cations. Such double-domain ligand strands are thus able to undergo a combined unfolding–folding interconversion on binding and release of metal cations. These changes can be modulated through coupling to a competing ligand that reversibly binds and releases metal cations, when respectively unprotonated and protonated, on effecting alternate pH changes. The resulting process thus performs nanomechanical extension/contraction molecular motions of a linear motor type, which is fueled by acid–base neutralization.



## INTRODUCTION

The implementation of molecular and supramolecular nanodevices to perform controlled motions in response to physical stimuli or chemical effectors is challenging the creativity of chemists toward the design of so-called “molecular machines” (switches and motors). The high activity generated is reflected in the many reviews describing the work performed in this field.<sup>1</sup>

Molecular switches and motors are based on motional processes of various mechanical kinds, such as axial shuttling<sup>2</sup> or sliding, unidirectional axial rotation,<sup>3</sup> walking,<sup>4</sup> spring extension, coiling or wrapping (folding),<sup>5</sup> and others. Most of the devices reported until now undergo only one of the above-mentioned types of molecular motions. We report herein the synthesis and the study of the motional features of a new type of nanomechanical molecular device, which performs simultaneously two kinds of motions in a correlated fashion within the same molecular framework in a sole motional operation. Such a behavior has been achieved by the design of ligand strands 1–3, presenting a linear domain connected to a helically folded one, which, on binding of metal ions, undergo helical wrapping of the linear part and extension of the helical domain into a linear one. Conversely, on removal of the metal ions by trapping with a competing ligand, the opposite processes occur, thus restoring the initial shapes of the free ligand strands. This type of system thus represents a hybrid motional device that is capable of performing a reversible wrap/unwrap process resulting in correlated simultaneous contraction/extension motions. It produces a kind of reversible worm-like motion, on binding and removal of

metal ions. The structural formulas of the double-domain (linear and helical) oligo-heterocyclic molecular strands 1–3, discussed herein, are given below (Figure 1).

**Rationale and Design Principles.** The design of the present molecular entities capable of performing coupled motions of different types is based on our earlier work on the control of the shape of polyheterocyclic strands by means of “folding codons” (“foldons”)<sup>6</sup> consisting of a specific sequence of aza-aromatic heterocyclic group. In our laboratory, we have earlier designed and synthesized such helical shape-persistent polyheterocyclic strands<sup>7a–d</sup> based on helicity-enforcing sequences of  $\alpha,\alpha'$ -connected pyridine-pyrimidine (py-pym) units that behave as helicity codon. The folding features are based on the strong preference of  $\alpha,\alpha'$ -bipyridine (by about 25–30 kJ/mol)<sup>8</sup> for the *transoid* conformation about the C–C bond in the N=C–C=N fragment rather than for the *cisoid* one. On the other hand and for the same reasons, sequences of  $\alpha,\alpha'$ -connected pyridine groups present a linear shape.<sup>9</sup> In view of the isomorphism between a pyridine group and a hydrazone unit (as described earlier),<sup>10</sup> the same bias is expected to hold for the analogous sequences incorporating hydrazone units, hydrazone-pyridine (hyz-py), hydrazone-pyrimidine (hyz-pym), as well as hydrazone-pyrazine (hyz-pz). Thus, whereas hyz-pym units are bent and encode helical strands,<sup>10,11</sup> hyz-py units generate strands of linear geometry.<sup>12</sup> Figure 2 illustrates the

Received: August 23, 2013

Published: February 18, 2014

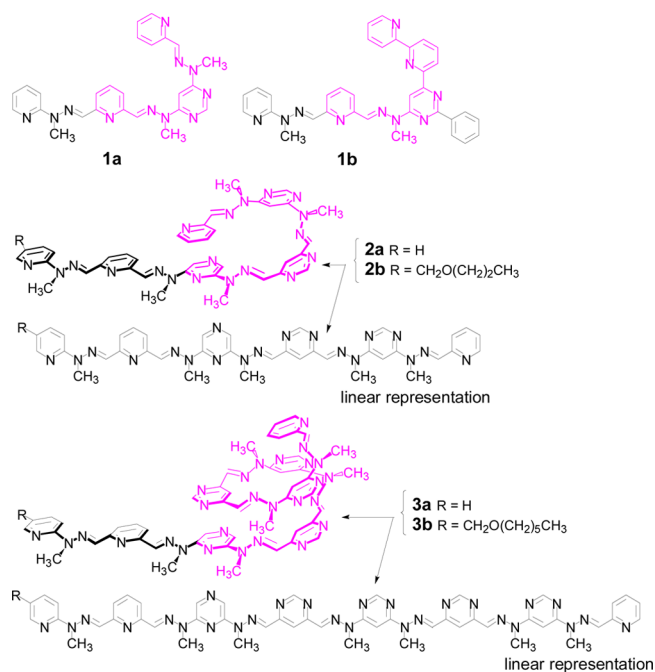


**Figure 1.** Formulas of ligands 1–3. Bent/helical part, in magenta.

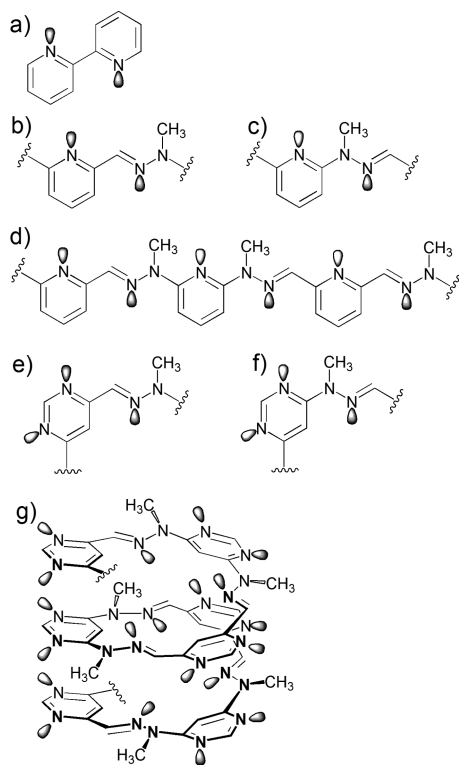


**Figure 2.** Conformational preferences of several heterocycle-heterocycle and combined hydrazone-heterocycle motifs and sequences: (a) 2,2'-bipyridine; (b) pyridine-2-hydrazone derived from pyridine-2-aldehyde; (c) pyridine-2-hydrazone derived from pyridine-2-hydrazine; (d) oligomeric pyridine-hydrazone sequence; (e) pyrimidine-4-hydrazone derived from pyrimidine-4-aldehyde; (f) pyrimidine-4-hydrazone derived from pyrimidine-4-hydrazine; and (g) helical oligomeric pyrimidine-hydrazone sequence.

structural features of these hyz-pym and hyz-py units and of derived sequences.

Complexation with appropriate metal ions occurs with conversion of the *transoid* form of the free ligand to the *cisoid* one.

As a consequence, helical strands based on (py-pym)<sup>13</sup> as well as on hydrazone-pyrimidine (hyz-pym)<sup>14</sup> units are uncoiled/unfolded on metal ion binding and thus generate linear polynuclear complexes. Conversely, on metal ion complexation, the linear conformation of (py-hyz)-based ligand strands is converted into a helical one wrapped around the cation(s).<sup>7e,f,12</sup> Such interconversions can be operated reversibly by introducing a competing ligand and have been integrated into pH-triggered motional devices that function through reversible binding and release of metal ions fueled by sequential acid–base neutralizations.<sup>12,13,14a,15</sup> The motions generated may be of very large amplitudes, for instance, of a factor of 6 (from a helix of about 11 Å height to a strand of ca. 60 Å length).<sup>14a</sup> The motional function accomplished by the helical ligands on binding of metal ions is an extension into a linear shape, while, conversely, the linear ligand strands under the same conditions perform a contraction on folding into a helical shape. In addition, in the latter case, the folding around the metal ions generates an entity that may be considered as a substrate-induced channel-like architecture, potentially able to display a (highly selective) transport function.<sup>16</sup> These shape changes are represented schematically in Figure 3.

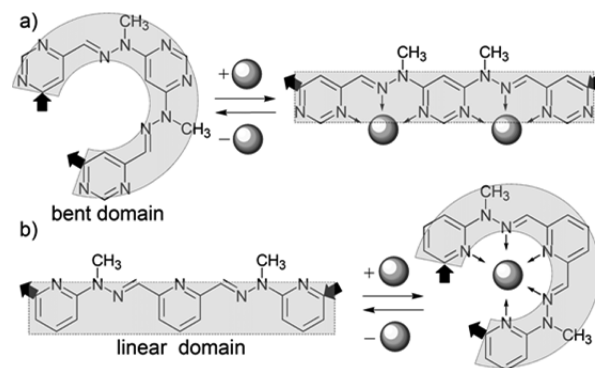


**Figure 3.** Shape changes induced by coordination of metal ions to (a) bent pym-hyz-pym-hyz-pym sequence producing a linear conformation of the ligand, and (b) linear py-hyz-py-hyz-py sequence producing a bent/circular/helical conformation of the ligand. The combination of these shape modulation effects is at the basis of the coupled molecular motions reported herein.

Several types of direct connection of the linear and helical domains can be envisaged for the construction of bimodal strands, as illustrated in Figure 4. Connections through spacers

Modes of direct connection between linear and helical (bent) strands

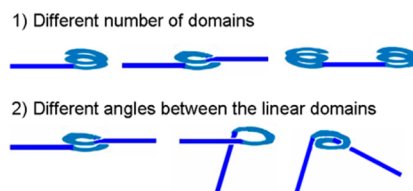


**Figure 4.** Types of possible connections between a helical domain and a linear domain in a molecular strand.

can also be considered. In particular, polymeric entities could, for instance, involve alternating helical and linear domains and undergo very large changes in length on metal ion complexation.

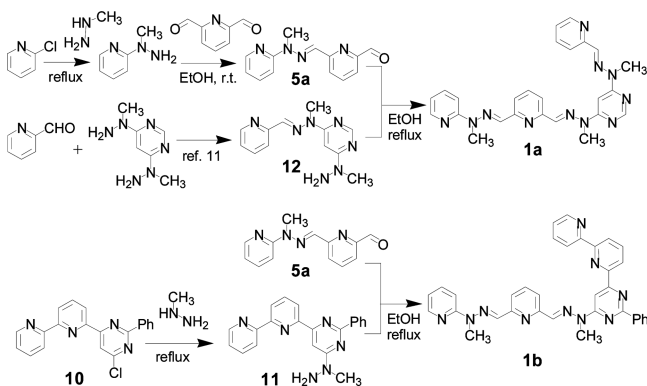


Figure 5. Synthesis of ligand strands 1a,b.

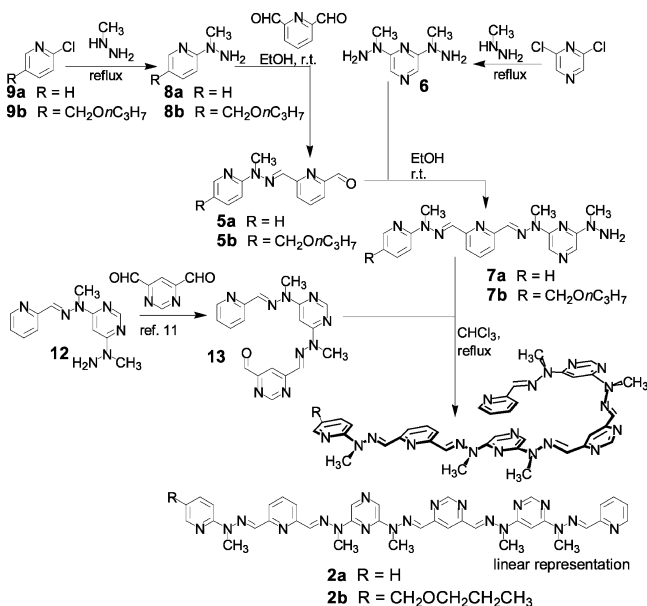


Figure 6. Synthesis of ligand strands 2a,b.

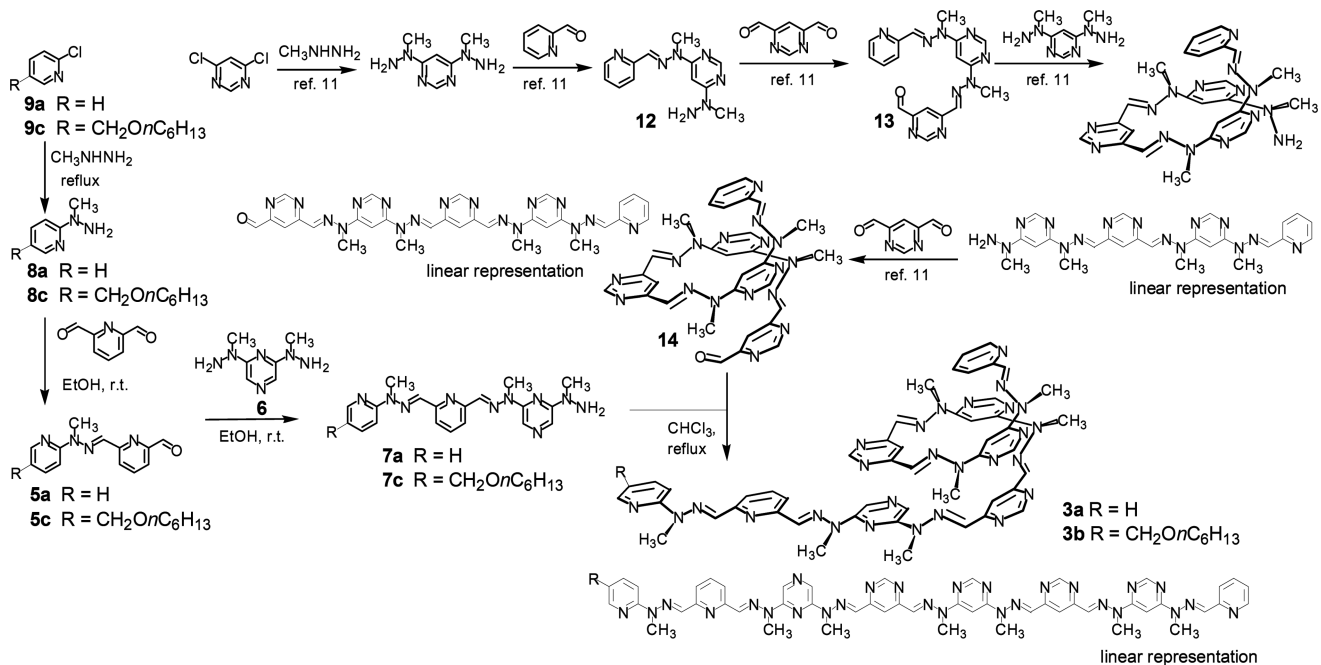


Figure 7. Synthesis of ligand strands 3a,b.

Each type of linear-helical connection shown in Figure 4 represents a category of motional devices combining simultaneously two different metal-ion induced shape changes that can be performed independently by the linear and helical strands alone. Thus, direct connection of the two domains leads to a new type of device presenting correlated motions with novel nanomechanical features. These motions, as described here, involve morphological changes triggered by a metal-supramolecular interaction without change in the constitution of the entity undergoing motion, that is, motional dynamics without constitutional dynamics.<sup>6</sup> Motional processes may also be merged with covalent constitutional changes.<sup>17,18</sup> In the present case, the incorporation of hydrazone functionalities in the molecular strands 1–3 allows in principle also for performing such covalent constitutional modification.

## RESULTS AND DISCUSSION

**Synthesis and Structure of the Ligand Strands.** For the synthesis of the present bidomain ligands, we took advantage of the isomorphic replacement of a 2,6-pyridine unit by the hydrazone group<sup>10,11</sup> (as indicated above), which gives much easier synthetic access to the desired strands and opens new perspectives for more sophisticated classes of ligands.

Concerning the synthetic strategy, it is possible to design and synthesize the mixed strands that contain both a linear and a circular (helical) domain through a step-by-step sequential process, by successively connecting the required heterocycles through hydrazone units. It is also possible to separately synthesize the linear and helical domains and then to connect them in the final step in a convergent process. On the basis of our previous experience, we decided to follow the last strategy (Figures 5, 6, and 7). The precursors 12–14 were synthesized as previously reported.<sup>11</sup> The linear domains were derived from the condensation of pyridine-2,6-dicarboxaldehyde with a pyridine-2-hydrazine and pyrazine-2,6-dihydrazine. The synthetic procedures are described in the Supporting Information.

Thus, mixed helical-linear strands containing three, five, and seven hydrazone groups have been synthesized. NOESY and

ROESY 2D NMR techniques have been used to ascertain the conformation of ligands in solution. For example, for ligand **1a**, the proton–proton correlations due to NOE effects, especially for the pairs of protons (4,8), (8,11), (4,11), and (13,16), as well as cross peaks between CH<sub>3</sub> and CH protons of hydrazone groups confirm the hybrid, linear and bent/circular, conformation of **1a** (Figure 8). Similar data hold for the strands of

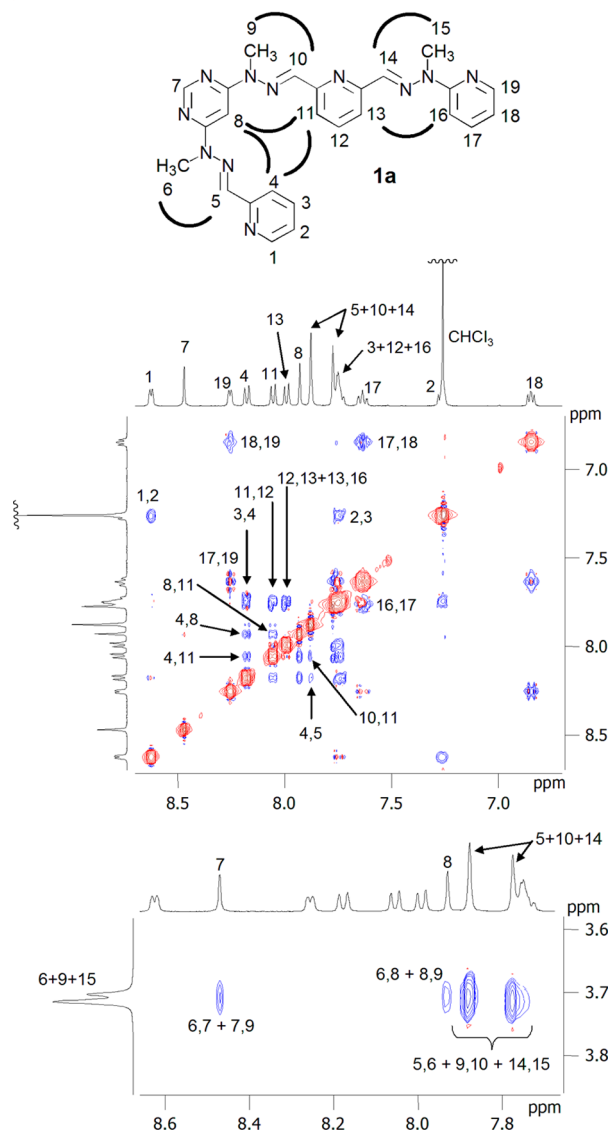


**Figure 8.** 400 MHz proton <sup>1</sup>H NMR NOESY spectrum of ligand **1a** (solvent CDCl<sub>3</sub>). Key cross peaks are indicated on the formula as circular arcs.

types **2** and **3** (see the Supporting Information). The cross peaks of lower intensity (4,5) and (10,11) may suggest a small torsion angle between the HC=N group and the pyridine ring connected to it. In the X-ray structures of previously reported hydrazone-pyrimidine-based helical ligands,<sup>11</sup> distances similar to those between protons 4 and 5 are of about 3.6 Å, and distances similar to those between protons 4 and 8 and protons 8 and 11 generally range between 2.9 and 3.3 Å.

In the solid state, the helicity of the domains based on sequences of hyz-pym subunits has been confirmed by X-ray crystallography in previous studies.<sup>10,11</sup> To demonstrate the linearity of ligands based on hyz-py sequences, we obtained,

after unsuccessful attempts with unsubstituted bishydrazone-strands, single crystals of compound **4**, bearing a phenyl group on each of its two terminal pyridines (Figure 9). The linear

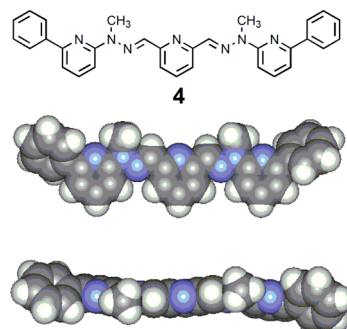


**Figure 9.** X-ray structure of the linear ligand **4** consisting of a sequence pyridine-hydrazone-pyridine-hydrazone-pyridine.

shape of the sequence py-hyz-py-hyz-py is clearly apparent. The distances between the Nsp<sup>2</sup> atoms of the hyz groups in transoid conformation are of 7 Å.

Increasing the number of heterocycles leads to a decrease in the solubility of the strands. To improve the solubility, as required for performing studies of reversible molecular motions in homogeneous systems, a CH<sub>2</sub>O-alkyl group has been attached to one of the terminal pyridine rings of the linear domains in **2b** and **3b**.

**Structural Changes on Complexation of Metal Cations.** On coordination of metal ions, the hyz-py and hyz-pym groups must undergo a change from the *transoid* to the *cisoid* conformation, to generate tridentate coordination subunits (Figure 3). As a consequence, cation binding to the ligand strands produces the uncoiling of the circular or bent domain<sup>13,14</sup> and the coiling of the linear one.<sup>12</sup> The corresponding structural changes are represented schematically for strands **2** and **3** in Figure 10. While the connecting fragment that is common to both domains (cd or fh) will not move, the other sections of the ligands undergo a large structural change on binding and removal of metal ions. Thus, a part (ad or hg) of the folded domain (adc or fhg) of the free ligand becomes part of the linear domain of the complex, while a part (bc or ef) of the linear domain (bcd or efh) of the free ligand becomes part of the folded domain of the complex.

The shape changes undergone by the ligand strands **1**, **2**, and **3** on binding and removal of metal cations are shown in Figure 11 in the molecular structure representation. Thus, treatment of the ligands **1**, **2**, and **3** with 2, 3, and 5 equiv of Pb(OTf)<sub>2</sub>, respectively (usually, an excess of 10–30%), leads to the complexes **1–Pb**<sub>2</sub>, **2–Pb**<sub>3</sub>, and **3–Pb**<sub>5</sub>. The subunits py-hyz-py, py-hyz-pym, and pym-hyz-pym generate cation binding sites that can be seen as terpyridine analogues. Each unit binds one Pb(II) cation in the linear domain, whereas in the helical part the ligand wraps around the cation in a pseudomacrocyclic fashion (see also Figure 3).

The conformational changes occurring can be observed by NOESY or ROESY <sup>1</sup>H NMR. Cross peaks corresponding to NOE (nuclear Overhauser effect) or ROE (NOE in the rotating frame) between the protons of the –NCH<sub>3</sub>– groups and the protons located at β position on the heterocycle (Figure 12a) or between the proton of –N=CH– groups and the protons located in β on the corresponding heterocycle (Figure 12b) are characteristic of the complexes. Together with the NOE or ROE

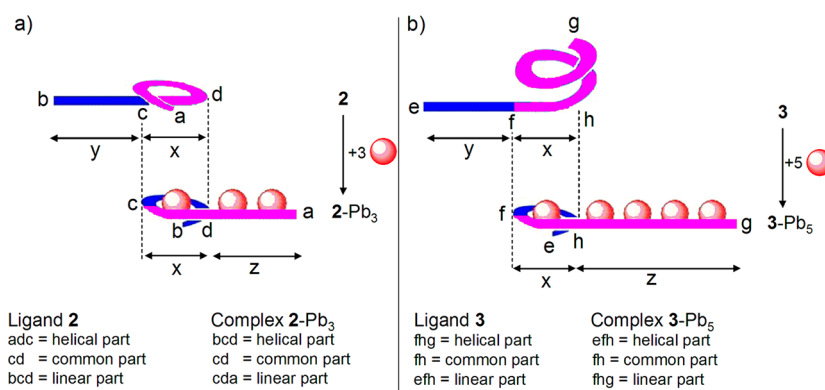


**Figure 10.** Schematic representations of the structural changes undergone by the bidomain ligands **2** and **3** on formation of the corresponding complexes with three and five cations, respectively.

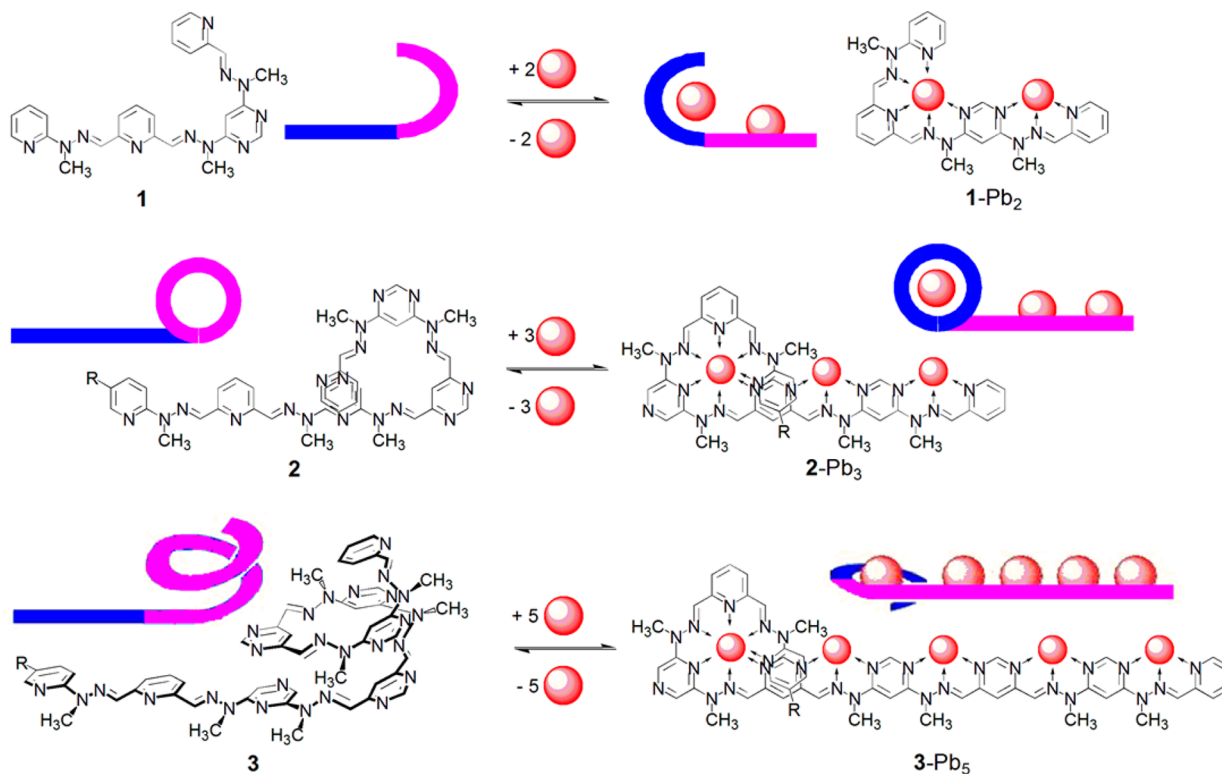


**Figure 11.** Reaction of ligands **1a** (top), **2** (middle), and **3** (bottom) with 2, 3, and 5 equiv of Pb(OTf)<sub>2</sub>, as necessary for the binding of the required number of Pb<sup>2+</sup> ions to the coordination subunits in the strands.

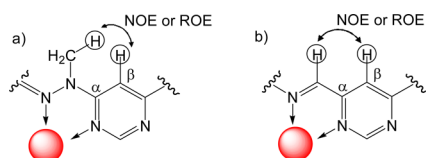


**Figure 12.** Key NOE or ROE interactions in the complexes formed by ligands **1–3** (see also Figure 11).

between methyl protons and the CH proton in the hydrazone unit  $\text{--NCH}_3\text{--N=CH--}$  that are also present in the ligands, the NOE or ROE data confirm the expected conformation of the coordinated ligands in the Pb(II) complexes. For example, these kinds of NOE (Figure 13) or ROE have been observed in the NOESY or ROESY spectra of the complexes.

X-ray crystallographic studies on single crystals of complexes **1a–Pb<sub>2</sub>**, **1b–Pb<sub>2</sub>** (Figure 14), and **2a–Pb<sub>3</sub>** (Figure 15)

confirmed, in the solid state, the structures and shapes predicted above on the basis of conformational principles and deduced from the analysis of the NMR data. The Pb–Pb distances are of 6.95 Å in complex **1a–Pb<sub>2</sub>**, of 7.11 Å in **1b–Pb<sub>2</sub>**, and of 6.61 and 7.36 Å in complex **2a–Pb<sub>3</sub>**, comparable to the Pb–Pb distances observed in the stick- or rack-like Pb(II) complexes reported by us earlier.<sup>13,14</sup>

In **1a–Pb<sub>2</sub>**, the unit between the pyrimidine and the terminal pyridine is a hydrazone, while in **1b–Pb<sub>2</sub>** it is a pyridine, and in both complexes **1a–Pb<sub>2</sub>** and **1b–Pb<sub>2</sub>** the overall shape of the heterocyclic strands is similar (Figure 14a,d). This is in agreement with the isomorphous equivalence between a 2,6-disubstituted pyridine and a hydrazone. In **1b–Pb<sub>2</sub>**, a terminal pyridine overlaps partially with the phenyl ring at position 2 of pyrimidine, and so the bent part of the coordinated ligand **1b** is of helical nature (Figure 14d–g). The angle between the planes of phenyl

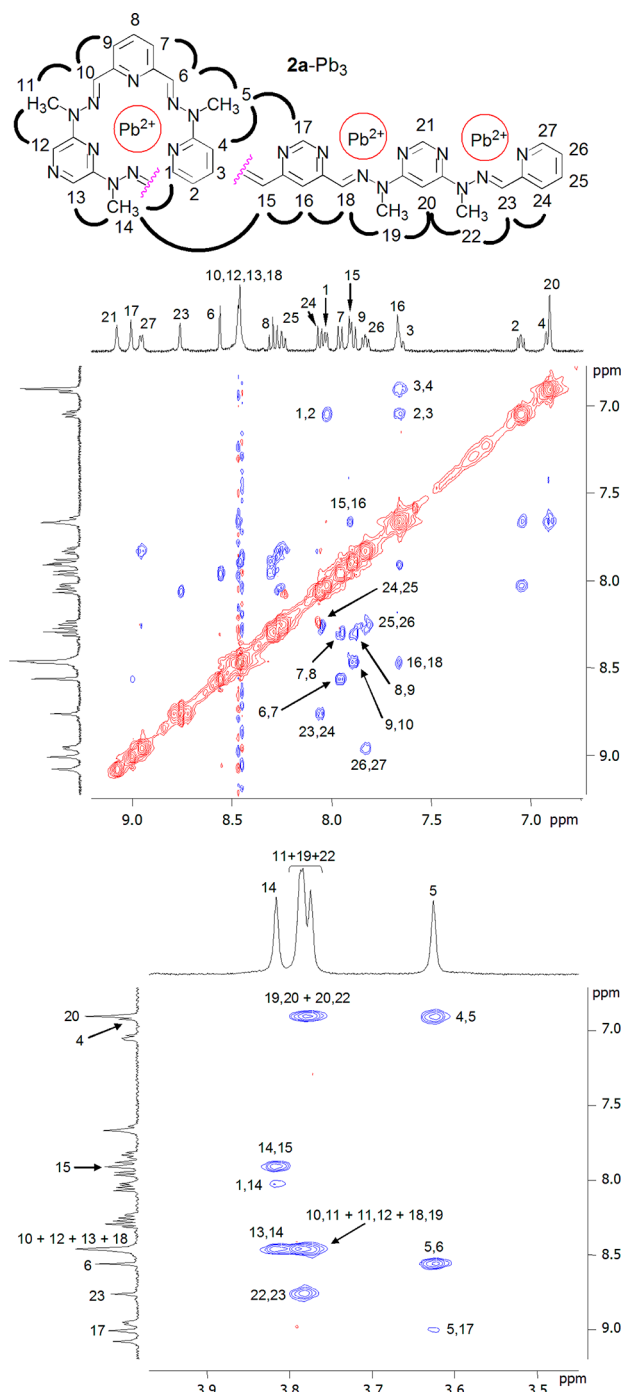


**Figure 13.** 400 MHz proton  $^1\text{H}$  NMR NOESY spectrum of complex  $2\text{a-Pb}_3$  in  $\text{CD}_3\text{CN}$ . Key cross peaks are indicated on the formula as circular arcs.

ring and pyridine is of  $33.8^\circ$ , the centroid-to-centroid distance between the two rings is of  $4.5 \text{ \AA}$ , and the distance between the proton at position 6 of the pyridine and the centroid of the phenyl is of  $3 \text{ \AA}$  (Figure 14g).

In the solid state,  $1\text{a-Pb}_2$  has a polymeric structure where the complexes are connected through triflate anions (Figure 14c).

The coordination spheres ( $< 3 \text{ \AA}$ ) of  $\text{Pb}^{2+}$  ions within the crystals of complexes are of type  $\text{N}_3\text{O}_3$  (three  $\text{N}_{\text{sp}^2}$  atoms and three triflates) and  $\text{N}_5\text{O}_3$  (five  $\text{N}_{\text{sp}^2}$  atoms and three triflates) for  $1\text{a-Pb}_2$ , of type  $\text{N}_3\text{O}_3$  (three  $\text{N}_{\text{sp}^2}$  atoms and three triflates) and  $\text{N}_5\text{O}_2$  (five  $\text{N}_{\text{sp}^2}$  atoms and two triflates) for  $1\text{b-Pb}_2$ , and of type

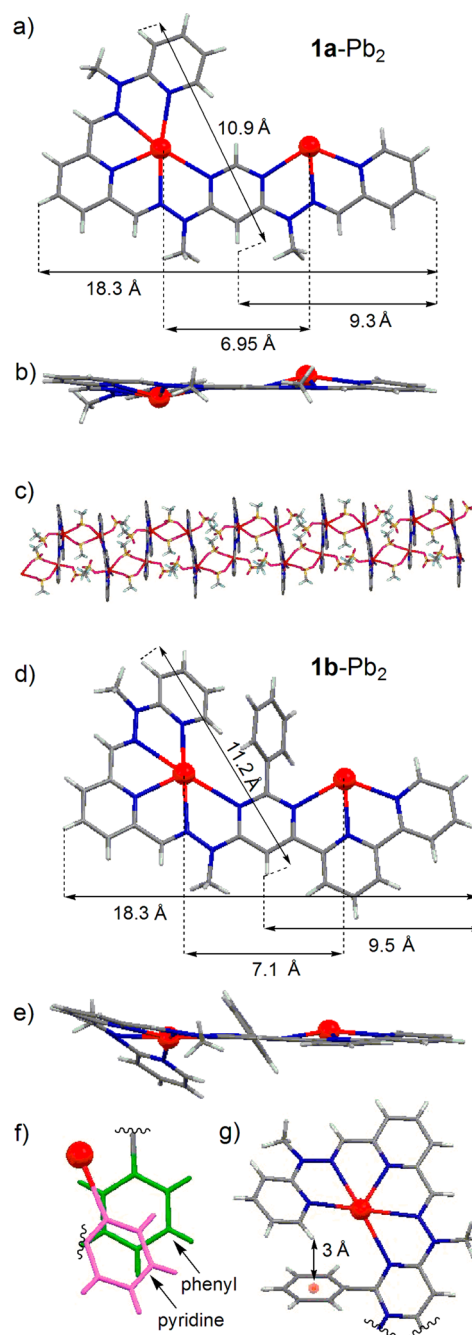


**Figure 14.** X-ray crystallographic solid-state structure of the complexes  $1\text{a-Pb}_2$  (views perpendicular (a) and parallel (b) to the main plane of the ligand; polymeric structure in the solid state (c)) and  $1\text{b-Pb}_2$  (views perpendicular (d) and parallel (e) to the main plane of the ligand; partial overlap between phenyl and pyridine rings (f); distance between the proton at position 6 of pyridine and the centroid of the phenyl ring (g)). Anions and solvent were omitted for clarity.

$\text{N}_8\text{O}$  (seven  $\text{N}_{\text{sp}^2}$  atoms, one molecule of acetonitrile, and one triflate),  $\text{N}_4\text{O}_3$  (three  $\text{N}_{\text{sp}^2}$  atoms, one molecule of acetonitrile, two triflates, and one molecule of water), and  $\text{N}_3\text{O}_3$  (three  $\text{N}_{\text{sp}^2}$  atoms and three triflates) for  $2\text{a-Pb}_3$ .

The helical domain of complex  $2\text{a-Pb}_3$  has a helical pitch of about  $3.5\text{--}4 \text{ \AA}$ , and its linear domain has a length of about  $25 \text{ \AA}$ . The total length of the ligand  $2\text{a}$  is of about  $40 \text{ \AA}$ , of which 63% belongs to the folded helix (circular part and common part), the remaining 37% being the unfolded section. The dimensions of the complex  $3\text{-Pb}_3$  can be estimated (Table 1) on the basis

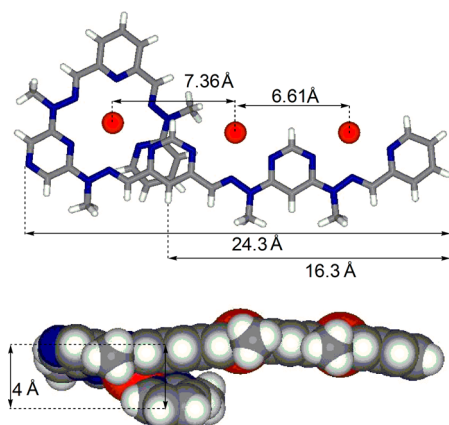
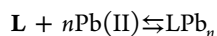


**Figure 15.** X-ray crystallographic solid-state structure of the complex **2a**–Pb<sub>3</sub>: (top) ball-and-stick, (bottom) space-filling representations; anions and solvent molecules were omitted for clarity.

of the structural data obtained for **1a**–Pb<sub>2</sub> and **2a**–Pb<sub>3</sub>. The total length of the strand should be of about 54 Å. In the complex, 46% (about 25 Å) belongs to the folded domain, the other 54% (29 Å) being unfolded and containing four metal ions.

**Coupled Nanomechanical Motions Generated by Cation-Induced Structural Interconversion.** The introduction of a competing ligand allows for inducing the reversible shape changes depicted in Figure 11 for ligands **1**–**3** on binding and removal of metal ions, as shown earlier for single domain ligands performing just one type of motion.<sup>12,13,14a,15</sup> In this way, correlated, domain-specific, extension/contraction nanomechanical motions can be generated with the bidomain ligands **1**–**3**.

(1) The reaction of the free ligand strands **L** with the appropriate number of equivalents (or an excess) of Pb(II) produces the bidomain complex **L**–Pb<sub>*n*</sub> (charges omitted for simplicity) as the first motional step of the functioning of the device.



(2) The addition to this equilibrium of a competing ligand that is a stronger binder of Pb(II) than the heterocyclic sites of the strand, such as tris(aminoethyl)amine (tren), removes the bound cations from the strand and regenerates its initial shape in the free state. Thus, addition of 1 equiv (or more) of tren

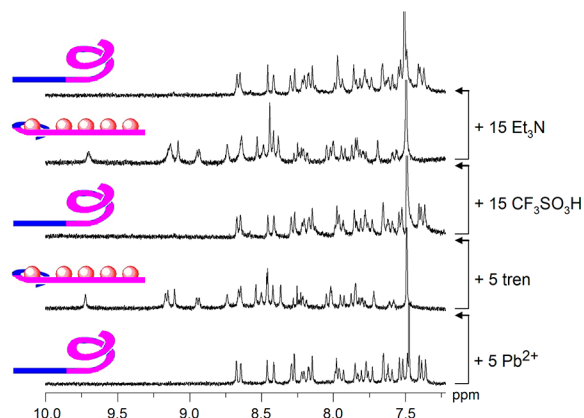
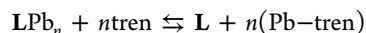
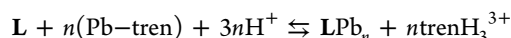


**Figure 17.** Partial aromatic region of the 300 MHz <sup>1</sup>H NMR spectra corresponding to a pH-modulated sequence of coupled motions of ligand **3b**, according to Figure 11 (starting solvent CDCl<sub>3</sub>/CD<sub>3</sub>CN 1/1 at 45°). See also the Supporting Information.

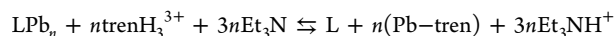
with respect to the amount of Pb(II) leads to the back conversion of each domain of the ligand to its initial shape in the free ligand.



(3) As the primary amine sites of tren are more basic than the heterocyclic nitrogen sites of the ligand strands, addition of trifluoromethanesulfonic (or triflic) acid CF<sub>3</sub>SO<sub>3</sub>H (3 equiv per equivalent of tren) to the solution containing the free ligand and the Pb–tren complex leads to protonation of tren (with formation of trenH<sub>3</sub><sup>3+</sup>) and release of Pb(II) ions that revert to binding again with the unprotonated bidomain ligand.



(4) Subsequent addition to this mixture of a base, such as Et<sub>3</sub>N, in suitable amount (e.g., 3 equiv (or an excess) of base per equivalent of tren) causes deprotonation of trenH<sub>3</sub><sup>3+</sup> to give tren that again can pick up the Pb(II) ions from the bidomain complex, thus regenerating the free ligand.



(5) The sequence of steps can be repeated, so that the system produces correlated nanomechanical motions triggered by pH changes and fueled by the acid–base neutralization energy. The process is represented in Figure 16 for ligand **2**.

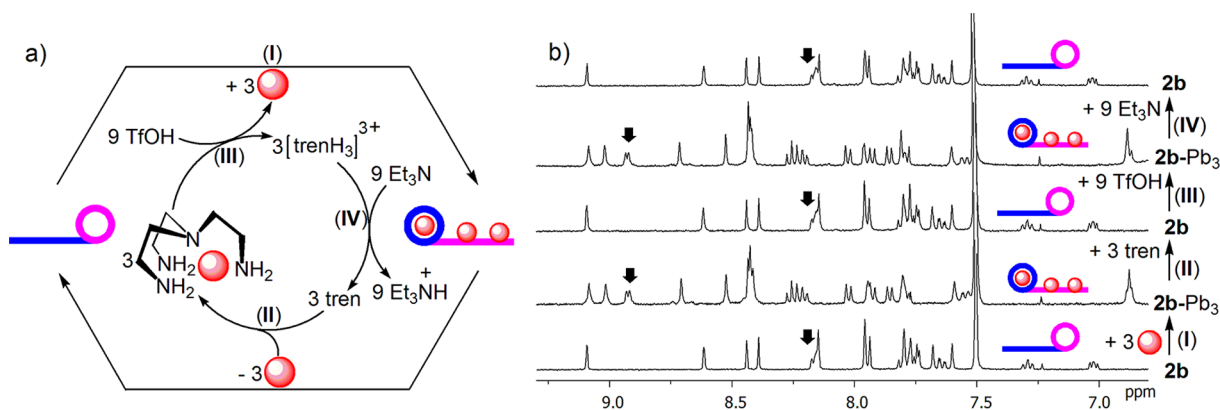


**Figure 16.** (a) Schematic representation of the pH-triggered correlated nanomechanical motions produced by helical/linear bidomain ligands, such as **2**. The process is fueled by acid–base neutralization. The red spherical objects are metal cations, here Pb(II). (b) The <sup>1</sup>H NMR monitoring of the process in the case of ligand **2b** (a part of the aromatic region is shown; starting solvent CDCl<sub>3</sub>/CD<sub>3</sub>CN 2/3; 400 MHz).

Table 1. Mechanical Parameters of the Motional Processes<sup>a</sup>

ligand	<i>x</i>	<i>y</i>	<i>z</i>	total length of the strand ( <i>x+y+z</i> )	distance between the ends of linear domain before complexation	distance between the ends of linear domain after complexation	coiling amplitude	distance between the ends of helical domain before complexation	distance between the ends of helical domain after complexation	uncoiling amplitude
1	10	8	8	26	18	9	9	9	18	9
2	10	15	15	40	25	4	21	4	25	21
3	10	15	29	54	25	4	21	9	39	30

<sup>a</sup>All lengths (average, rounded to whole values) are in angstroms. See Figure 10. For ligand 1, the bent instead of the helical domain is considered. The linear domain of the free ligand becomes, after complexation, the helical domain of the complex; the helical domain of the free ligand becomes, after complexation, the linear domain of the complex.

It involves the uncoiling of a circular/helical domain coupled with the coiling of a linear domain. The motions can be followed by NMR as shown in Figure 17 for ligand 3b.

In this coupled uncoiling/coiling process, two amplitudes are to be considered: the folding amplitude and the unfolding amplitude. They can be calculated as the difference between the ends of each domain in its two states, coiled and uncoiled (Table 1). For ligands 2 and 3, all amplitudes are of at least 20 Å (Table 1).

The energetic aspects of the coiling/uncoiling process of the type of those occurring in strands 1–3 have been analyzed earlier for single domain helical ligands.<sup>14a</sup> A similar analysis can be attempted for the present bidomain strands, although the situation is more complicated due to the simultaneous operation of coiling and uncoiling in the same strand. In our previous work, it was estimated that the energy corresponding to the change from the uncoordinated conformation of a pyrimidine-hydrazone-pyrimidine subunit to its form in the coordinated state present in the Pb<sup>2+</sup> complexes was, without taking into account the coordination energy, of about 60 kJ·mol<sup>-1</sup>. Thus, for ligands of type 1, 2, and 3, containing, respectively, 3, 5, and 7 such hydrazone subunits per molecule, this energy can be estimated to amount to about 180, 300, and 420 kJ mol<sup>-1</sup>, respectively. The energy of the process that corresponds to the above conformational change together with the coordination of a Pb<sup>2+</sup> ion was estimated at -47 kJ mol<sup>-1</sup> per pyrimidine-hydrazone-pyrimidine subunit. For ligands 1, 2, and 3, this estimation then leads to -141, -235, and -329 kJ mol<sup>-1</sup>, respectively.

## CONCLUSION

We have reported herein the design and behavior of a molecular system representing a nanomechanical motional device based on molecular ligand strands capable of undergoing coupled changes in shape on binding and release of metal cations. It displays the following remarkable features.

The first is a bidomain structure: the strands are composed of two directly connected sections, a linear unfolded one and a folded helical one, whose shapes are strongly enforced by the conformational preferences of the heterocyclic/heteroatomic subunits of which they are constituted.

Next is a bidomain functionality: the strands act as ligands for metal cations. On coordination of metal cations, the components of the strands undergo a conformational change, which induces coupled shape changes in the two sections of the strands. The linear part folds into a bent/helical shape, wrapping around the bound metal ion(s), thus generating also a self-induced channel-like domain. Conversely and simultaneously, the helical domain uncoils and produces a stick-like complexed domain. The process results in a unique coupled, contraction/extension motion, reminiscent of the correlated

action of muscles in the arm, where both motions also occur simultaneously.

The complementary contraction/extension shape changes induced by the interaction with metal ions result in nanomechanical motions of particularly large amplitude.

These motions can be generated reversibly by coupling with a competing ligand, which allows for cation removal and release, modulated through alternate addition of acid and base and fueled by acid–base neutralization. An integrated version of the present systems might be considered by directly grafting the competing ligand group to the molecular strand.

One may envisage that the double motional behavior of molecules such as those described here could be implemented to perform displacements on a surface, whereby the ends of the bidomain strand would be alternately connected and disconnected from the support, for instance, by using orthogonal functional groups such as imine and disulfide.

Multiple structural and functional features are prominent in biomolecules, in multidomain proteins.<sup>19</sup> One may also note the analogy between the motions described herein and the reptation modes of DNA molecules, as observed by fluorescence microscopy<sup>20</sup> (Figure 18). The structures of the two molecules

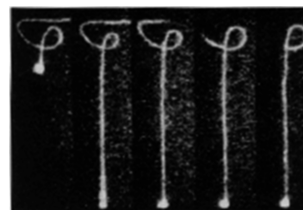


Figure 18. Reptation of DNA molecules, as observed by fluorescence microscopy. Reprinted with permission from ref 20. Copyright 1994 AAAS.

as well as the causes of their motions are different, but the natures of the motions (uncoiling of a coiled part and coiling of a linear part) are formally similar in both cases.

In the general framework of the design of complex chemical systems, molecules presenting two or more structural and/or functional domains allow for the development of processes and networks of increased complexity, presenting features such as coupling, control, and feedback.<sup>21</sup>

## ASSOCIATED CONTENT

### Supporting Information

Experimental procedures, NMR spectra, and CIF files. This material is available free of charge via the Internet at <http://pubs.acs.org>. The CIF files for this Article have been deposited at the Cambridge Crystallographic Data Centre, and they

have been assigned the following deposition numbers: 773968 (1a-Pb<sub>2</sub>), 957474 (1b-Pb<sub>2</sub>), 773969 (2a-Pb<sub>3</sub>), and 957475 (4).

## AUTHOR INFORMATION

### Corresponding Authors

lehn@unistra.fr; mstadler@unistra.fr

### Notes

The authors declare no competing financial interest.

## ACKNOWLEDGMENTS

We wish to dedicate this work to Jack Roberts on the occasion of his 95th birthday, in recognition of his outstanding contributions to the world of chemistry over so many years. We thank the Université de Strasbourg and the CNRS (UMR 7006) for financial support. We thank Dr. Lydia Brelot, Corinne Bailly, and Dr. André DeCian for X-ray crystallographic studies, Dr. Bruno Vincent, Dr. Lionel Allouche, Jean-Daniel Sauer, Dr. Jean-Louis Schmitt, and Maurice Coppe for assistance with NMR experiments, and Mélanie Lebreton and Dr. Héléne Nierengarten for mass spectrometry analyses.

## REFERENCES

- (1) For reviews, see: (a) Balzani, V.; Credi, A.; Raymo, F. M.; Stoddart, J. F. *Angew. Chem., Int. Ed.* **2000**, *39*, 3349–3391. (b) *Acc. Chem. Res.* **2001**, *34*, 409–522 (special issue on molecular machines). (c) Sauvage, J.-P., Ed. *Structure and Bonding. Molecular Machines and Motors*; Springer: Berlin, 2001. (d) Balzani, V.; Venturi, M.; Credi, A. *Molecular Devices and Machines. A Journey into the Nanoworld*; Wiley-VCH: Weinheim, 2003. (e) Kottas, G. S.; Clarke, L. I.; Horinek, D.; Michl, J. *Chem. Rev.* **2005**, *105*, 1281–1376. (f) Kinbara, K.; Aida, T. *Chem. Rev.* **2005**, *105*, 1377–1400. (g) Kay, E. R.; Leigh, D. A. In *Functional Artificial Receptors*; Schrader, T., Hamilton, A. D., Eds.; Wiley-VCH: Weinheim, 2005; pp 333–406. (h) Kelly, T. R., Ed. *Topics in Current Chemistry*; Springer: Berlin, 2005. (i) Klaffer, J.; Urbakh, M., Eds. *J. Phys.: Condens. Matter* **2005**, *17*, S3661–S4024. (j) Leigh, D. A.; Zerbetto, F.; Kay, E. R. *Angew. Chem., Int. Ed.* **2007**, *46*, 72–191. (k) Kinosita, K., Jr.; Shiroguchi, K.; Ali, M. Y.; Adachi, K.; Itoh, H. *Adv. Exp. Med. Biol.* **2007**, *592*, 369–384. (l) Benson, C. R.; Share, A. I.; Flood, A. H. In *Bioinspiration and Biomimicry in Chemistry*; Swiegers, G. F., Ed.; Wiley: Hoboken, NJ, 2012; Chapter 4, pp 71–119.
- (2) (a) Anelli, P. L.; Spencer, N.; Stoddart, J. F. *J. Am. Chem. Soc.* **1991**, *113*, 5131–5133. (b) Armaroli, N.; Balzani, V.; Collin, J.-P.; Gaviña, P.; Sauvage, J.-P.; Ventura, B. *J. Am. Chem. Soc.* **1999**, *121*, 4397–4408. (c) Cao, J.; Fyfe, M. C. T.; Stoddart, J. F. *J. Org. Chem.* **2000**, *65*, 1937–1946. (d) Leigh, D. A.; Pérez, E. M. *Chem. Commun.* **2004**, 2262–2263. (e) Abe, Y.; Okamura, H.; Nakazono, K.; Koyama, Y.; Uchida, S.; Takata, T. *Org. Lett.* **2012**, *14*, 4122–4125. (f) Durot, S.; Reviriego, F.; Sauvage, J.-P. *Dalton Trans.* **2010**, *39*, 10557–10570.
- (3) (a) Kelly, T. R.; De Silva, H.; Silva, R. A. *Nature* **1999**, *401*, 150–152. (b) Kelly, T. R.; Silva, R. A.; De Silva, H.; Jasmin, S.; Zhao, Y. *J. Am. Chem. Soc.* **2000**, *122*, 6935–6949. (c) Flechter, S. P.; Dumur, F.; Pollard, M. M.; Feringa, B. L. *Science* **2005**, *310*, 80–82. (d) Koumura, N.; Geertsema, E. M.; Meetsma, A.; Feringa, B. L. *J. Am. Chem. Soc.* **2000**, *122*, 12005–12006. (e) Koumura, N.; Geertsema, E. M.; van Gelder, M. B.; Meetsma, A.; Feringa, B. L. *J. Am. Chem. Soc.* **2002**, *124*, 5037–5051. (f) van Delden, R. A.; Koumura, N.; Harada, N.; Feringa, B. L. *Proc. Natl. Acad. Sci. U.S.A.* **2002**, *99*, 4945–4949. (g) van Delden, R. A.; Koumura, N.; Schoevaars, A.; Meetsma, A.; Feringa, B. L. *Org. Biomol. Chem.* **2003**, *1*, 33–35.
- (4) von Delius, M.; Geertsema, E. M.; Leigh, D. A. *Nat. Chem.* **2010**, *2*, 96–101.
- (5) (a) For a photoswitchable foldamer, see: Khan, A.; Kaiser, C.; Hecht, S. *Angew. Chem., Int. Ed.* **2006**, *45*, 1878–1881. (b) For examples of reversible uncoiling by protonation, see: Dolain, C.; Maurizot, V.; Huc, I. *Angew. Chem., Int. Ed.* **2003**, *42*, 2738–2740.

- (c) Kolomiets, E.; Berl, V.; Odriozola, I.; Stadler, A.-M.; Kyritsakas, N.; Lehn, J.-M. *Chem. Commun.* **2003**, 2868–2869. (d) For folding by interaction with metal ions, see, for example: Prince, R. B.; Okada, T.; Moore, J. S. *Angew. Chem., Int. Ed.* **1999**, *38*, 233–236. (e) For folding by interaction with anions, see, for example: Xu, Y.-X.; Wang, G.-T.; Zhao, X.; Jiang, X.-K.; Li, Z.-T. *J. Org. Chem.* **2009**, *74*, 7267–7273. (f) For reviews on folding, see, for example: Hill, D. J.; Mio, M. J.; Prince, R. B.; Hughes, T. S.; Moore, J. S. *Chem. Rev.* **2001**, *101*, 3893–4011. (g) Goodman, C. M.; Choi, S.; Shandler, S.; DeGrado, W. F. *Nat. Chem. Biol.* **2007**, *3*, 252–262. (h) Juwarker, H.; Suk, J.-M.; Jeong, K.-S. *Chem. Soc. Rev.* **2009**, *38*, 3316–3325. (i) Guichard, G.; Huc, I. *Chem. Commun.* **2011**, *47*, 5933–5941.
- (6) (a) Lehn, J.-M. *Angew. Chem., Int. Ed.* **2013**, *52*, 2836–2850. (b) Lehn, J.-M. *Top. Curr. Chem.* **2012**, *278*, 1–32.
- (7) (a) Hanan, G. S.; Lehn, J.-M.; Kyritsakas, N.; Fischer, J. *J. Chem. Soc., Chem. Commun.* **1995**, 765–766. (b) Bassani, D. M.; Lehn, J.-M.; Baum, G.; Fenske, D. *Angew. Chem., Int. Ed. Engl.* **1997**, *36*, 1845–1847. (c) Ohkita, M.; Lehn, J.-M.; Baum, G.; Fenske, D. *Chem.—Eur. J.* **1999**, *5*, 3471–3481. (d) Ohkita, M.; Lehn, J.-M.; Baum, G.; Fenske, D. *Chem.—Eur. J.* **1999**, *5*, 3471–3481. (e) For recent reviews on the general theme of helical metal complexes, see: *Metallofoldamers*; Maayan, G., Albrecht, M., Eds.; Wiley: Chichester, 2013. (f) Maayan, G. *Eur. J. Org. Chem.* **2009**, 5699–5710.
- (8) Calculations yield a preference of 2,2'-bipyridine for the *transoid* with respect to *cisoid* form by about 25–30 kJ/mol: (a) Howard, S. T. *J. Am. Chem. Soc.* **1996**, *118*, 10269–10274. (b) Göller, A.; Grummt, U.-W. *Chem. Phys. Lett.* **2000**, *321*, 399–405. (c) Corongiu, G.; Nava, P. *Int. J. Quantum Chem.* **2003**, *93*, 395–405. For structural and spectroscopic data, see: (d) Merritt, L. L., Jr.; Schroeder, E. D. *Acta Crystallogr.* **1956**, *9*, 801–804. (e) Bertinotti, F.; Liquori, A. M.; Pirisi, R. *Gazz. Chim. Ital.* **1956**, *86*, 893–898. (f) Nakamoto, K. *J. Phys. Chem.* **1960**, *64*, 1420–1425. (g) Castellano, S.; Gunther, H.; Ebersole, S. *J. Phys. Chem.* **1965**, *69*, 4166–4176. (h) Calder, I. C.; Spotswood, T. M.; Tanzer, C. I. *Aust. J. Chem.* **1967**, *20*, 1195–1212. (i) Barone, V.; Minichino, C.; Fliszar, S.; Russo, N. *Can. J. Chem.* **1988**, *66*, 1313–1317. (j) Jaime, C.; Font, J. *J. Org. Chem.* **1990**, *55*, 2637–2644.
- (9) Potts, K. T.; Raiford, K. A. G.; Keshavarz-K, M. *J. Am. Chem. Soc.* **1993**, *115*, 2793–2807.
- (10) Gardinier, K. M.; Khoury, R. G.; Lehn, J.-M. *Chem.—Eur. J.* **2000**, *6*, 4124–4131.
- (11) Schmitt, J.-L.; Stadler, A.-M.; Kyritsakas, N.; Lehn, J.-M. *Helv. Chim. Acta* **2003**, *86*, 1598–1624.
- (12) Stadler, A.-M.; Kyritsakas, N.; Lehn, J.-M. *Chem. Commun.* **2004**, 2024–2025.
- (13) Barboiu, M.; Lehn, J.-M. *Proc. Natl. Acad. Sci. U.S.A.* **2002**, *99*, 5201–5206.
- (14) (a) Stadler, A.-M.; Kyritsakas, N.; Graff, R.; Lehn, J.-M. *Chem.—Eur. J.* **2006**, *12*, 4503–4522. (b) For other examples of linear complexes of hydrazone-pyrimidine-based ligands, see: Hutchinson, D. J.; Hanton, L. R.; Moratti, S. C. *Inorg. Chem.* **2010**, *49*, 5923–5934. (c) Hutchinson, D. J.; Hanton, L. R.; Moratti, S. C. *Inorg. Chem.* **2011**, *50*, 7637–7649. (d) Hutchinson, D. J.; Cameron, S. A.; Hanton, L. R.; Moratti, S. C. *Inorg. Chem.* **2012**, *51*, 5070–5081. (e) Hutchinson, D. J.; Hanton, L. R.; Moratti, S. C. *Inorg. Chem.* **2013**, *52*, 2716–2728.
- (15) (a) Barboiu, M.; Vaughan, G.; Kyritsakas, N.; Lehn, J.-M. *Chem.—Eur. J.* **2003**, *9*, 763. (b) Stadler, A.-M.; Kyritsakas, N.; Vaughan, G.; Lehn, J.-M. *Chem.—Eur. J.* **2007**, *13*, 59–68. (c) Stadler, A.-M.; Ramirez, J.; Lehn, J.-M. *Chem.—Eur. J.* **2010**, *16*, 5369–5378.
- (16) (a) Sakai, N.; Matile, S. *Angew. Chem., Int. Ed.* **2008**, *47*, 9603. (b) Fyles, T. M. *Chem. Soc. Rev.* **2007**, *36*, 335. (c) Matile, S.; Som, A.; Sorde, N. *Tetrahedron* **2004**, *60*, 6405.
- (17) Kovářiček, P.; Lehn, J.-M. *J. Am. Chem. Soc.* **2012**, *134*, 9446–9455.
- (18) For a review on molecular motional processes involving covalent changes, see: Stadler, A.-M.; Ramirez, J. *Top. Curr. Chem.* **2012**, *322*, 261–290.

(19) For an analysis of the folding and evolution of multidomain proteins, see: Han, J.-H.; Batey, S.; Nickson, A. A.; Teichmann, S. A.; Clarke, J. *Nat. Rev.* **2007**, *8*, 319–330.

(20) Perkins, T. T.; Smith, D. E.; Chu, S. *Science* **1994**, *264*, 819–822.

(21) For two unrelated examples of multidomain operation, see, for instance: (a) Funeriu, D. P.; Lehn, J.-M.; Fromm, K. M.; Fenske, D. *Chem.—Eur. J.* **2000**, *6*, 2103–2111. (b) See also Figure 2 in: Lehn, J.-M. *Top. Curr. Chem.* **2012**, *322*, 1–32. (c) Ichinose, W.; Shigeno, M.; Yamaguchi, M. *Chem.—Eur. J.* **2012**, *18*, 12644–12654.